

Rotons of composite fermions: Comparison between theory and experiment

Vito W. Scarola, Kwon Park, and Jainendra K. Jain

Department of Physics, 104 Davey Laboratory, The Pennsylvania State University, University Park, Pennsylvania 16802

(Received 27 December 1999)

This paper reports results of our comprehensive theoretical study of the rotons of composite fermions. The calculated roton energies at Landau-level fillings of $1/3$, $2/5$, and $3/7$ are in excellent agreement with the energies measured in inelastic light scattering and ballistic phonon absorption experiments.

I. INTRODUCTION

Interacting electrons in the lowest Landau level capture an even number of flux quanta to form a quantum fluid of composite fermions, which has been the subject of intense investigation over the last decade.¹⁻³ At certain special filling factors this fluid is incompressible, which results in the phenomenon of the fractional quantum Hall effect (FQHE).⁴ This paper is concerned with the neutral excitations of the incompressible states of composite fermions. These were first observed by Pinczuk and co-workers^{5,6} by inelastic light scattering at a filling factor $\nu=1/3$, and subsequently by several groups by light^{7,8} as well as ballistic phonon⁹⁻¹¹ scattering at other filling factors as well (e.g., at $\nu=2/5$, $2/3$, and $3/7$).

Theoretically, the neutral excitations of the FQHE were first considered by Girvin, MacDonald, and Platzman (GMP)¹² in 1985. By analogy to the Feynman-Bijl wave function for the collective excitation of superfluid ^4He ,

$$\chi_k^{FB} = \chi_0 \sum_j e^{-i\mathbf{k}\cdot\mathbf{r}_j} \quad (1)$$

they considered the so-called single-mode-approximation (SMA) variational wave function

$$\chi_k^{SMA} = \mathcal{P}_{LLL} \chi_0 \sum_j e^{-i\mathbf{k}\cdot\mathbf{r}_j} \quad (2)$$

for the neutral excitation of incompressible fractional quantum Hall effect (FQHE) states, which will be referred to below as the GMP mode. Here χ_0 is the ground state wave function, $\sum_j e^{-i\mathbf{k}\cdot\mathbf{r}_j}$ is the density operator, \mathbf{k} is the wave vector, \mathbf{r}_j is the position of the j th particle, and \mathcal{P}_{LLL} is the lowest Landau level (LL) projection operator. The dispersion obtained from this was shown to have a finite energy in the limit of small wave vectors, and to possess a minimum at a finite wave vector, where the neutral excitation is called the ‘‘roton,’’ again by analogy to ^4He . Rotons are of special significance in the FQHE since they are the lowest-energy excitations, there being no phononlike massless mode at small wave vectors, and therefore determine the low temperature thermodynamics of the FQHE. We shall see below that the wave function χ_k^{SMA} is a reasonable approximation at $\nu=1/3$ at small to intermediate wave vectors, but it is inadequate at filling fractions other than $1/3$. Interestingly, the roton energy predicted by the Feynman-Bijl wave function

χ_k^{FB} for ^4He was also not accurate, being off by a factor of 2 compared to experiment, but after incorporating backflow corrections¹³ and further improvements,¹⁴ an excellent agreement with experiment was obtained, which is recognized as one of the major triumphs of the theory of ^4He . No backflow correction is required for the wave function in Eq. (2),¹² and it is not clear how one might go about modifying it. We will see that an understanding of the physics of the ground state contains the clue to the resolution of this puzzle.

A different principle for obtaining the wave function of the neutral excitation suggested itself within the framework of the composite fermion (CF) theory of the fractional quantum Hall effect.^{3,1,2} A composite fermion is the bound state of an electron and an even number of magnetic flux quanta (a flux quantum is defined as $\phi_0=hc/e$), formed when electrons confined to two dimensions are exposed to a strong magnetic field. According to this theory, the interacting electrons at the Landau-level filling factor $\nu=n/(2pn\pm 1)$, n and p being integers, transform into weakly interacting composite fermions at an effective filling $\nu^*=n$; the ground state corresponds to n filled CF-LL's, and the neutral excitation to a particle-hole pair of composite fermions, called the CF exciton. We shall see that the CF exciton in general has several minima in its dispersion; at the lowest-energy minimum the neutral excitation is called the fundamental CF roton (or simply the CF roton), and the other minima are known as the secondary CF rotons. The Jain wave functions for the CF ground state and the CF exciton are constructed by analogy to the wave functions of the electron ground state at filling factor n , Φ_n^{gs} , and its exciton, Φ_n^{ex} :

$$\Psi_{n/(2pn+1)}^{gs} = \mathcal{P}_{LLL} \prod_{j<k} (z_j - z_k)^{2p} \Phi_n^{gs}, \quad (3)$$

$$\Psi_{n/(2pn+1)}^{ex} = \mathcal{P}_{LLL} \prod_{j<k} (z_j - z_k)^{2p} \Phi_n^{ex}, \quad (4)$$

where $z_j=x_j+iy_j$ is the position of the j th particle, and \mathcal{P}_{LLL} denotes the projection of the wave function into the lowest Landau level. Φ_n^{gs} and Φ_n^{ex} are constructed for non-interacting electrons, and are therefore fully known. $\Psi_{n/(2pn+1)}^{gs}$ and $\Psi_{n/(2pn+1)}^{ex}$ have been found to be extremely accurate in tests against exact diagonalization results available for small systems,^{3,15,16} which convincingly establish the validity of the CF exciton description of the lowest-energy neutral mode for *all* FQHE states in the lowest Lan-

dau level. Even at $\nu=1/3$, the CF roton energy is approximately 15–20% lower than that the lowest energy obtained in the SMA approach.¹

There have been two developments in recent years that have renewed interest in the question of the roton energy. First, and most important, there has been tremendous experimental progress in the measurement of the energy of the roton both by inelastic Raman scattering^{5–8} and by ballistic phonon absorption,^{9–11} and its energy has been determined at Landau-level fillings of 1/3, 2/5, and 3/7. Second, while the basic theoretical framework for the CF exciton has been in place since 1989, and many studies have established its validity over the years, it is only recently that it has become possible to deal with large systems needed for a reliable quantitative estimation of the roton energy. We have carried out a comprehensive calculation of the roton energy at several filling factors in the lowest Landau level. The finite transverse thickness of the electron wave function, which modifies the short-range part of the interaction between electrons as a function of the distance in the two-dimensional plane, has been incorporated through a self-consistent local-density approximation. We note that, to our knowledge, this is the first time that the roton energy has been calculated for a realistic interaction potential for any filling factor, and our study constitutes the most reliable comparison between theory and experiment even for the neutral excitation at $\nu=1/3$.

Another motivation for undertaking the present work is as follows. The Jain wave functions are in an extremely good quantitative accord with the idealized computer experiments (i.e., exact diagonalization studies on small systems), with the energies of the low-lying states obtained accurately at the level of 0.1%. The comparison with the real experiments is however not as satisfactory. Quantitative tests of the theory of the fractional quantum Hall effect have focused in the past primarily on the gap to *charged* excitation, namely, a far separated CF particle-hole pair, determined experimentally from the temperature dependence of the longitudinal resistance. It was believed for some time that after including the effects of transverse thickness and Landau-level mixing, the theory gives a decent account of the experimental gap at 1/3. This, in turn, was based on assertions that finite thickness causes almost a factor of 2 reduction in the gap, which is further decreased by 20–30% due to Landau level mixing; with these corrections the theoretical and experimental gaps were in reasonable agreement.¹⁷ However, a more careful investigation shows that the estimation of the magnitudes of the various corrections was oversimplified. First of all, the transverse thickness brings about a smaller reduction ($\sim 30\%$) of the gap than believed earlier.^{18,19} Second, Landau-level mixing is not as significant an effect for systems with a realistic width as it is for strictly two-dimensional systems;^{20,21} this can be understood from the fact that the short distance part of the effective interaction, which is primarily responsible for causing Landau-level mixing, becomes weaker due to the finite thickness. In early estimations it was incorrectly assumed that the two effects are additive, thereby overestimating the size of the net reduction in the gap. Recent calculations, believed to be more reliable, show a substantial discrepancy between theory and experiment even after finite thickness and Landau-level mix-

ing are taken into account.^{18,19} It is natural to suspect that this is caused by the ever-present disorder, for which no quantitatively reliable theoretical treatment is available at the moment.

It will therefore be useful to focus instead on quantities that are not very sensitive to disorder. What are these? Since the relevant disorder potential is caused by the charged donor ions, it is plausible that quantities that do not involve charged excitations will be less affected by disorder. One such example is that of transitions between different FQHE *ground* states at the same filling factor, as happens, for example, when the spin polarization of the ground state changes from one value to another as a function of the Zeeman energy.²² The other example is that of the CF roton. The disorder is not likely to affect its energy as significantly as it does the energy of the charged excitation, since the roton has a much weaker dipolar coupling to disorder due to its overall charge neutrality, and the coupling is further diminished because the disorder in modulation doped samples is typically smooth on the scale of the size (on the order a magnetic length) of the spatially localized roton. There is also compelling experimental evidence for the insensitivity of the roton energy to disorder:⁹ the same roton energy was found for samples for which the gaps in transport experiments differed by as much as a factor of 2.

Thus, apart from its importance in its own right, the roton provides a wonderful opportunity for testing the quantitative validity of our understanding of the excitations of the fractional quantum Hall state. We find that our calculated energy of the CF roton agrees with experiment typically at a level of 10%, which is quite satisfactory, especially given that there is no adjustable parameter in the calculation.

There have been other theoretical calculations of the dispersion of the CF exciton, especially using the framework of the Chern-Simons formulation of composite fermions.^{23,24} The results are in qualitative consistency with those obtained from the microscopic wave functions.

II. CALCULATIONAL METHOD

A. Wave functions

The spherical geometry^{25,26} will be used in our calculations, in which electrons move on the surface of a sphere under the presence of a radial magnetic field produced by a magnetic monopole at the center. The monopole strength will be denoted by Q , which can be either an integer or a half-integer according to Dirac's quantization condition, corresponding to a total flux of $2Qh/e$ through the surface of the sphere. The composite fermion theory maps the problem of interacting electrons at Q to that of composite fermions at $q=Q-p(N-1)$. The wave functions for interacting electrons at Q are then constructed as

$$\Psi_Q^{gs} = \mathcal{P}_{LLL} \Phi_1^{2p} \Phi_q^{gs} \quad (5)$$

and

$$\Psi_{Q,L}^{ex} = \mathcal{P}_{LLL} \Phi_1^{2p} \Phi_{q,L}^{ex}. \quad (6)$$

Here, Φ_q are Slater determinantal wave functions of noninteracting electrons at q , and Φ_1 is the wave function of the

fully occupied lowest Landau level written at a monopole strength $q_1 = (N-1)/2$, given by

$$\Phi_1 = \prod_{j < k} (u_j v_k - u_k v_j), \quad (7)$$

where $u_j \equiv \cos(\theta_j/2) \exp(-i\phi_j/2)$ and $v_j \equiv \sin(\theta_j/2) \exp(i\phi_j/2)$. The single-particle eigenstates at q are called the monopole harmonics,²⁶ which are given by¹⁵

$$Y_{q,n,m}(\mathbf{r}_j) = N_{q,n,m} (-1)^{q+n+m} e^{iq\phi_j} u_j^{q-m} v_j^{q+m} \sum_{s=0}^n (-1)^s \times \binom{n}{s} \binom{2q+n}{q+n+m-s} (v_j^* v_j)^{n-s} (u_j^* u_j)^s, \quad (8)$$

where $n=0,1,\dots$ is the Landau-level index, $l=q+n$ is the orbital angular momentum, and m is the z component of the orbital angular momentum. The normalization coefficients are

$$N_{q,n,m} = \left[\frac{(2q+2n+1)(q+n+m)!(q+n-m)!}{4\pi(2q+n)!} \right]^{1/2}. \quad (9)$$

The wave functions for noninteracting electrons are written in terms of Slater determinants constructed from $Y_\alpha(\mathbf{r}_j)$,

$$\text{Det}[Y_\alpha(\mathbf{r}_j)], \quad (10)$$

where α collectively denotes q, n , and m . It was shown earlier that the process of multiplication by Φ_1^{2p} followed by lowest Landau-level projection is tantamount to substituting the single-electron wave functions $Y_\alpha(\mathbf{r}_j)$ in Φ_q by the single CF wave functions $Y_\alpha^{CF}(\mathbf{r}_j)$, defined as¹⁶

$$Y_\alpha^{CF}(\mathbf{r}_j) = \mathcal{P}_{LLL} \prod_k (u_j v_k - u_k v_j)^p Y_\alpha(\mathbf{r}_j), \quad (11)$$

where the prime signifies the condition $k \neq j$. Applying the projection operator yields¹⁶

$$Y_{q,n,m}^{CF}(\mathbf{r}_j) = J_j^p e^{iq\phi_j} \left[\frac{[2q+p(N-1)+1]!}{[2q+p(N-1)+n+1]!} \right] \times N_{q,n,m} (-1)^{q+n+m} u_j^{q-m} v_j^{q+m} \sum_{s=0}^n (-1)^s \binom{n}{s} \times \binom{2q+n}{q+n+m-s} v_j^{n-s} u_j^s [\bar{U}_j^s \cdot \bar{V}_j^{n-s} \cdot 1], \quad (12)$$

where

$$J_j \equiv \prod_k (u_j v_k - v_j u_k) e^{(i/2)(\phi_j + \phi_k)}, \quad (13)$$

$$\bar{U}_j \equiv p \sum_k \frac{v_k}{u_j v_k - v_j u_k} + \frac{\partial}{\partial u_j}, \quad (14)$$

and

$$\bar{V}_j \equiv p \sum_k \frac{-u_k}{u_j v_k - v_j u_k} + \frac{\partial}{\partial v_j}. \quad (15)$$

Using the single CF wave function as a correlated basis function, the wave functions of interacting electrons are written in terms of Slater determinants constructed from $Y_\alpha^{CF}(\mathbf{r}_j)$:

$$\text{Det}[Y_\alpha^{CF}(\mathbf{r}_j)]. \quad (16)$$

Note that due to the spherical symmetry, the total angular momentum L is a good quantum number; it is preserved in going from the state at q to the state at Q according to the prescription above, since the total angular momentum of Φ_1 is zero (it is a filled shell).

The wave function for the ground state at Q is obtained from the Slater determinantal wave function at q which corresponds to n filled Landau levels. In fact, this condition fixes the relation between Q and the number of particles for $\nu = n/(2n+1)$: n shells are filled for $q = (N-n^2)/2n$, which corresponds to $Q = (1+1/2n)N - (1+n/2)$ (assuming here and below that each electron captures *two* flux quanta, i.e., $p=1$). Of course, in the limit of large N , we obtain the desired filling factor $2Q/N \rightarrow n/(2n+1)$.

The wave function of the exciton $\Phi_{q,L}^{ex}$ is a linear combination of Slater determinants, each of which corresponds to a state obtained by exciting an electron in the m_h state of the topmost occupied LL to the m_e state of the lowest unoccupied LL. The z component of the total angular momentum can be chosen to be zero, with no loss of generality, so that $m_e = m_h$. Denoting the Slater determinant with a particle-hole excitation as $\Phi_q^{m_h}$, the exciton state with a definite total angular momentum L is given by

$$\Phi_{q,L}^{ex} = \sum_{m_h} \langle n_t + q, -m_h; n_t + q + 1, m_h | L, 0 \rangle \Phi_q^{m_h}, \quad (17)$$

where n_t is the LL index of the topmost occupied CF LL, and $m_h = -q - n_t, \dots, q + n_t$. The CF exciton state is obtained from it as explained earlier, by multiplying it by Φ_1^2 followed by lowest Landau-level projection, as in Eq. (6); the final outcome is to make in the above wave function the replacement $Y \rightarrow Y^{CF}$. It is completely determined from symmetry alone, i.e., does not contain any adjustable parameter. Note that the relative amplitudes of various Slater determinants (coherence factors) remain unchanged in going from the electron exciton at q to the CF exciton at Q .

It is convenient to present the results as a function of k , the wave vector of the planar geometry. Following the usual approach, we shall write $k = L/R$, where $R = \sqrt{Q}l_0$ is the radius of the sphere, and $l_0 = \sqrt{\hbar/eB}$ is the magnetic length.

B. Effective interaction

The Hamiltonian for the many electron system in a uniform magnetic field is given by

$$H = \frac{1}{2m_b} \sum_i \left(-i\hbar \bar{\nabla}_i + \frac{e\bar{A}(\mathbf{r}_i)}{c} \right)^2 + \frac{1}{2} \sum_{j \neq k} V(r_{jk}) + V_{e-b}, \quad (18)$$

where the vector potential $\vec{A}(\mathbf{r})$ is given by $(B/2)(-y, x, 0)$, B is the magnitude of magnetic field, m_b is the band mass of the electron, $V(r)$ is the effective two-dimensional electron-electron interaction, and V_{e-b} is the electron-background interaction, with the background assumed to be comprised of a uniform positive charge. In the limit of $B \rightarrow \infty$, the electrons are confined to the lowest Landau level; the kinetic energy becomes an irrelevant constant and drops out of the problem. In what follows, we will restrict the Hilbert space to the lowest Landau level except in our discussion of Landau-level mixing.

For a strictly two-dimensional system, $V^{2D}(r_{jk}) = e^2/(\epsilon|r_j - r_k|)$, where ϵ is the dielectric constant of the background material. As we will see, an important quantitative correction comes from the finite transverse extent of the electron wave function, which alters the form of the effective two-dimensional interaction at short distances. The effective interaction can be calculated straightforwardly from a knowledge of the transverse wave function $\xi(z)$:

$$V(r) = \frac{e^2}{\epsilon} \int dz_1 \int dz_2 \frac{|\xi(z_1)|^2 |\xi(z_2)|^2}{[r^2 + (z_1 - z_2)^2]^{1/2}}. \quad (19)$$

The transverse wave function ξ , in turn, is determined in a standard manner by self-consistently solving the Schrödinger and Poisson equations, taking into account the interaction effects through the local density approximation including the exchange correlation potential.²⁷ Two geometries, single heterojunction (also called triangular quantum well) and square quantum well, are considered due to their experimental relevance. To simplify the calculation, we assume that the electron wave function is confined entirely on the GaAs side of the heterojunction, which is a reasonably good approximation for deep confinement (for further details, see Ref. 19). It is stressed that neither the Jain state nor the effective interaction contains any adjustable parameters; the former depends only on the filling factor, while the latter is determined from a first principles, self-consistent local-density-approximation (LDA) calculation, with the two-dimensional density, the sample type (heterojunction or square quantum well), and the known sample parameters as the only input.

There are various sources of error in our results. The intrinsic error in the wave functions is a relatively small effect, as is the statistical uncertainty in our Monte Carlo calculations. The error in the thermodynamic extrapolation²⁸ is also quite small for 1/3 and 2/5 (on the order of 1–2%), but somewhat larger for 3/7 (~15%). This gives the level of accuracy of our results for the Coulomb interaction. For the realistic situation with finite thickness, an additional source of error is introduced by the approximations made in the determination of the effective interaction within the framework of the LDA, which have been estimated to be possibly as large as 20%.²⁹ The error quoted below in our results refers only to the statistical uncertainty in the Monte Carlo sampling and thermodynamic extrapolations.

C. Landau-level mixing

Another possibly significant effect is that of Landau-level mixing. There have been several studies of Landau-level mixing on the transport gap,^{20,21} and the corrections have

been estimated on the order of 5–10% for typical experimental parameters. We will extend the work of Melik-Alaverdian and Bonesteel²⁰ to estimate the effect of Landau-level mixing on the CF roton of the 1/3 state. This is the simplest method for treating Landau-level mixing, and will be sufficient for our purposes. In this approach, one considers a variational wave function which is a linear combination of the projected and unprojected wave functions,

$$\Psi_Q(\gamma) = (\mathcal{P}_{LLL} + \gamma)\Phi_1^2\Phi_q, \quad (20)$$

and fixes the parameter γ by minimizing the total energy. Now it is also necessary to compute the kinetic energy of the state. In this choice of the variational wave function, however, the ground state at $\nu=1/3$, there is no Landau-level mixing in since $\Phi_1^2\Phi_q$ is already in the lowest Landau level, so $\Psi_Q^{gs}(\gamma) = \Phi_1^2\Phi_q^{gs}$, apart from an overall normalization factor. The total energy as a function of γ ,

$$\bar{H}_\gamma = \frac{\langle \Psi(\gamma) | H | \Psi(\gamma) \rangle}{\langle \Psi(\gamma) | \Psi(\gamma) \rangle}, \quad (21)$$

requires matrix elements of H and unity with respect to the projected and the unprojected state. The direct matrix elements, e.g., $\langle \mathcal{P}_{LLL}\Phi_1^2\Phi_q | H | \mathcal{P}_{LLL}\Phi_1^2\Phi_q \rangle$ or $\langle \Phi_1^2\Phi_q | H | \Phi_1^2\Phi_q \rangle$, can be calculated in the Monte Carlo approximation, and will be denoted by \bar{H}_0 and \bar{H}_∞ . The cross elements, e.g., $\langle \mathcal{P}_{LLL}\Phi_1^2\Phi_q | H | \Phi_1^2\Phi_q \rangle$, can be written in terms of direct matrix elements by choosing, say, $\gamma=1$. This gives

$$\bar{H}_\gamma = \frac{(1-\gamma)\bar{H}_0 N_0 + \gamma\bar{H}_1 N_1 - \gamma(1-\gamma)\bar{H}_\infty N_\infty}{(1-\gamma)N_0 + \gamma N_1 - \gamma(1-\gamma)N_\infty}, \quad (22)$$

where

$$N_\gamma = \langle \Psi(\gamma) | \Psi(\gamma) \rangle. \quad (23)$$

The terms \bar{H}_1 and \bar{H}_∞ in Eq. (22) require calculating the kinetic energy of the unprojected CF wave function, $\Psi(\infty)$, because it has components in the higher, electronic Landau levels. The total kinetic energy on the sphere is given by²⁶

$$K = \frac{\hbar\omega_c}{2Q} \sum_{j=1}^N \left[\frac{-1}{\sin(\theta_j)} \frac{\partial}{\partial \theta_j} \left(\sin(\theta_j) \frac{\partial}{\partial \theta_j} \right) + \frac{1}{\sin^2(\theta_j)} \left(Q \cos(\theta_j) - i \frac{\partial}{\partial \phi_j} - Q \right)^2 \right] - \frac{N\hbar\omega_c}{2}, \quad (24)$$

where $\hbar\omega_c = eB/m_b$ is the electronic cyclotron energy. We evaluate $K\Psi(\infty)$ within each Monte Carlo step using standard techniques for evaluating derivatives numerically.

D. Monte Carlo

The energy of the exciton at $\nu = n/(2n+1)$,

$$\Delta^{ex} = \frac{\langle \Psi_\nu^{ex} | H | \Psi_\nu^{ex} \rangle}{\langle \Psi_\nu^{ex} | \Psi_\nu^{ex} \rangle} - \frac{\langle \Psi_\nu^{gs} | H | \Psi_\nu^{gs} \rangle}{\langle \Psi_\nu^{gs} | \Psi_\nu^{gs} \rangle}, \quad (25)$$

is computed by Monte Carlo methods in the spherical geometry.²⁵ Because moving a single particle at each step of the Monte Carlo changes the single CF wave function Y^{CF} for *all* particles, the wave function must be computed fully at each step. The exciton wave function is a linear superposition of $\sim N/n$ Slater determinants, but each of these differs from the ground state only in one row, and the clever techniques for upgrading Slater determinants³⁰ significantly reduce the computing time, enabling us to study reasonably large systems (up to 63 composite fermions were used in the present study). To elaborate on our updating technique, first let $[Y^{CF}]_{\alpha,j}^{gs}$ denote an element of the matrix for the Slater determinant describing the ground state at Q , i.e., Ψ_Q^{gs} . As before, α collectively indicates orbital quantum numbers. Also, let $\Psi_Q^{m_h}$ denote the composite fermion wave function with CF hole (CF particle) located in the m_h state of the $n_t(n_t+1)$ Landau level:

$$\Psi_Q^{m_h} = \mathcal{P}_{LLL} \Phi_1^2 \Phi_q^{m_h}. \quad (26)$$

Then we compute the excited state by writing

$$\Psi_Q^{m_h} = \sum_{j=1}^N Y_{n_t+1, m_h}^{CF}(\mathbf{r}_j) [\overline{Y^{CF}}]_{(n_t, m_h), j}^{gs} \Psi_Q^{gs}, \quad (27)$$

where $[\overline{Y^{CF}}]^{gs}$ is the transpose of the inverse matrix of $[Y^{CF}]^{gs}$. Then Eqs. (6) and (17) are combined to give

$$\Psi_{Q,L}^{ex} = \sum_{m_h} \langle n_t + q, -m_h; n_t + q + 1, m_h | L, 0 \rangle \Psi_Q^{m_h}. \quad (28)$$

This reduces the number of operations from $O(N^3)$ to $O(N^2)$.

The ground and excited state energies are evaluated sufficiently accurately to obtain a reasonable estimate for the gap, using up to 10^7 Monte Carlo steps of the Metropolis algorithm. Due to the lack of edges in the spherical geometry being studied, we expect that the gap will have a linear dependence on N^{-1} to leading order, which is borne out by our results. A linear extrapolation to the thermodynamic limit $N^{-1} \rightarrow 0$ is taken after correcting the energies for the finite size deviation of the density from its thermodynamic value, which amounts to multiplying the chord distance by the factor $\sqrt{\rho_N/\rho} = \sqrt{N/2Q\nu}$, where ρ is the density in the thermodynamic limit and ρ_N is the density for the N particle system.³¹ In other words, the chord distance $2R|u_i v_j - u_j v_i|$ between two electrons on the sphere (R being the radius of the sphere) is identified with the thermodynamic distance

$$|r_i - r_j| = l_0 \sqrt{\frac{2N}{\nu}} |u_i v_j - u_j v_i|. \quad (29)$$

The LDA interaction $V_{LDA}(|r_i - r_j|)$ is determined for an infinite planar system, and the above prescription is used in evaluating the interaction energy in our Monte Carlo calculations in the spherical geometry. All results below are thermodynamic extrapolations, unless mentioned otherwise. The energies are quoted in units of $e^2/\epsilon l_0$.

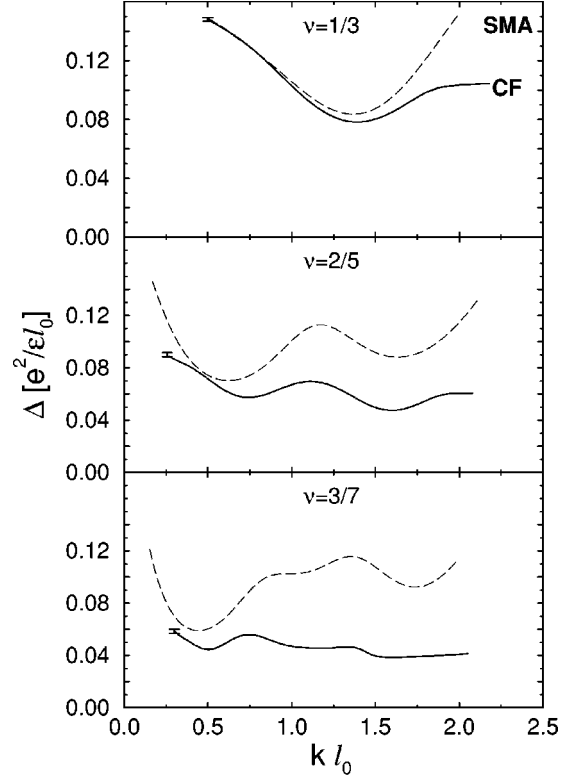


FIG. 1. The dispersions of the CF exciton at $\nu = 1/3, 2/5,$ and $3/7$ for the pure Coulomb interaction $V(r) = e^2/\epsilon r$. The solid curves are the dispersion curves for the CF exciton obtained from discrete points of finite systems, with the typical Monte Carlo uncertainty shown at the beginning of each curve, while the dashed curve is the dispersion of the GMP mode obtained in the single-mode approximation (SMA). The results for $1/3$ are for 8 particles, with the SMA results taken from S. He *et al.* [Phys. Rev. B **50**, 1823 (1994)]. For $2/5$ and $3/7$, the dispersion of the CF exciton is determined from a study of systems of up to 50 particles (without extrapolation to the thermodynamic limit; the extrapolation is shown in later figures), whereas that of the GMP mode is the thermodynamic limit, taken from Park and Jain (Ref. 32). The energies are given in units of $e^2/\epsilon l_0$, where $\epsilon = 12.8$ is the dielectric constant of GaAs, and l_0 is the magnetic length.

III. RESULTS

The dispersion of the CF exciton for $1/3, 2/5,$ and $3/7$ is shown in Fig. 1 for the pure Coulomb interaction $V(r) = e^2/\epsilon r$. Also shown for comparison is the dispersion of the GMP mode obtained in the single mode approximation.³² (The SMA requires a knowledge of the ground-state wave function; the wave function Ψ^{gs} was used for this purpose. Thus the same ground state is used for both the CF exciton and the GMP mode, and any energy difference between them comes entirely from the use of different wave functions for the excitation.) It has been known that the SMA does not describe the lowest energy excitation for large wave vectors ($kl_0 > 1$).¹² (We note, however, that the GMP mode is likely to be of experimental significance, and may appear as a broad additional peak in inelastic light scattering experiments.³²) We find that even at small wave vectors the CF exciton has a lower energy than the GMP mode, although the difference here is less dramatic.³³

It is illuminating to discuss in what physical sense Ψ_k^{ex}

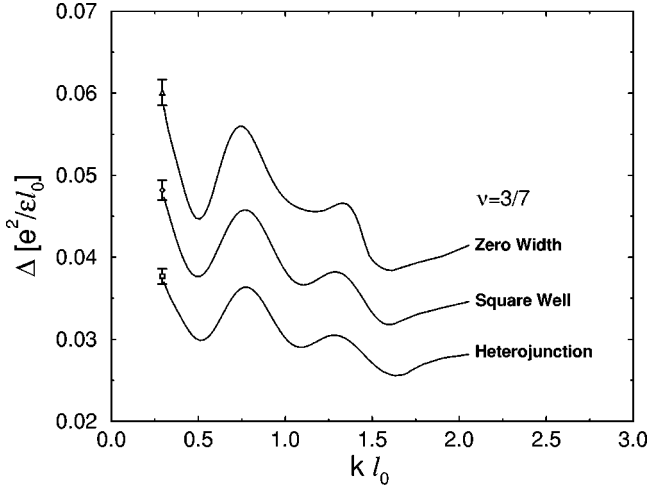


FIG. 2. The dispersions of the CF exciton at $\nu=3/7$ for a zero width system, for a heterojunction (with density $1.5 \times 10^{11} \text{ cm}^{-2}$), and for a square quantum well of width 30 nm (with density $0.5 \times 10^{11} \text{ cm}^{-2}$). The dispersions are for a system of 63 composite fermions, obtained by interpolation through the discrete k values available in the study.

and χ_k^{SMA} are different. The latter treats all electrons in the ground states in an equivalent manner, whereas the former excites only a composite fermion from the topmost Landau level. This clarifies why the two are most similar at $1/3$ [in fact, identical in the limit of $k \rightarrow 0$ (Ref. 34)] where only one

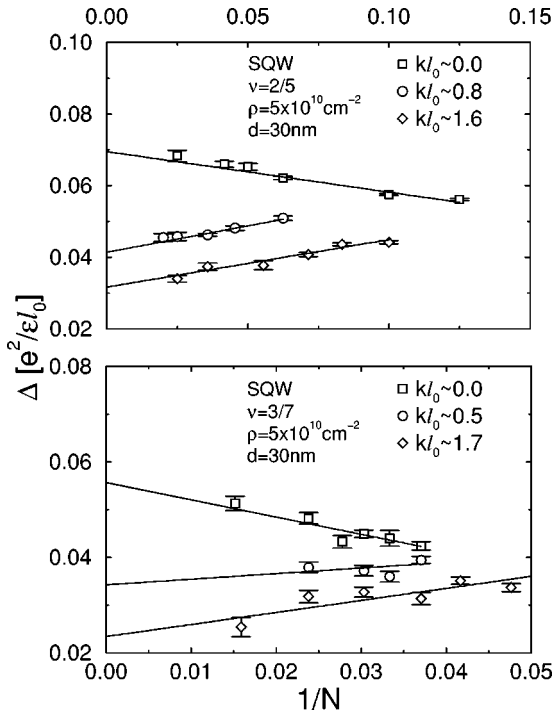


FIG. 3. N dependence of the energies of the fundamental and secondary CF rotons (diamonds and circles) and of the exciton energy in the long-wavelength limit (squares). For each N , the energy of the rotons is obtained by fitting a parabola through three or more points in the vicinity of the minimum. The energy in the thermodynamic limit is ascertained by a linear fit through the energies as a function of $1/N$. The parameters correspond to the experiment of Kang *et al.* (Ref. 7).

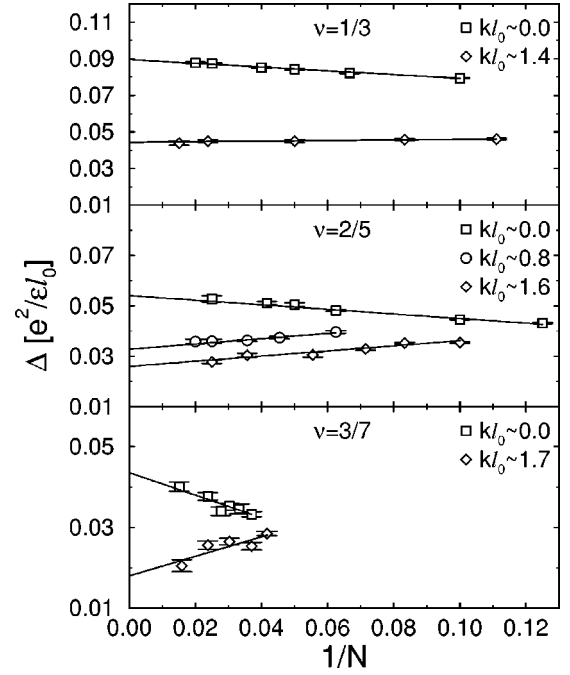


FIG. 4. N dependence of the energies of certain fundamental and secondary CF rotons (diamonds and circles), and of the exciton energy in the long-wavelength limit (squares) for a heterojunction sample with electron density $\rho=1.5 \times 10^{11} \text{ cm}^{-2}$. The parameters correspond to an experiment of Mellor *et al.*⁹

CF LL is occupied. Further, in χ_k^{SMA} the application of the density operator degrades the correlations in the ground state, but in Ψ^{ex} the correlations between electrons (through the Jastrow factor) are built in *after* creating the excitation in Φ_n , which, as shown by our results, is a more accurate approach. It is not surprising that an understanding of the physics of the ground state is crucial for an understanding of the excitations as well.

Figure 2 shows that the finite thickness of the wave function reduces the energy of the exciton significantly. Of special interest are the energy of the CF exciton in the limit $kl_0 \rightarrow 0$ and the energies of the fundamental and secondary rotons. The thermodynamic limit of these energies are obtained by an extrapolation of the energies obtained from finite systems, as shown in Figs. 3 and 4. Since only discrete values of k are available at finite N , the energy of the roton is

TABLE I. Energies of the CF roton and the long-wavelength neutral excitation at $1/3$, $2/5$, and $3/7$, for a strictly two-dimensional system, in units of $e^2/\epsilon l_0$. Also given is an estimate for the CF roton ‘‘mass,’’ $m_R^* \equiv \mu_R^* m_e \sqrt{B[T]}$, defined in Eq. (30), where m_e is the electron mass in vacuum. The statistical uncertainty in the last digit(s) is shown in parentheses.

| Mode | ν | Energy | μ_R^* |
|----------|-------|----------|------------|
| $kl_0=0$ | 1/3 | 0.15 | - |
| | 2/5 | 0.087(1) | - |
| | 3/7 | 0.068(5) | - |
| roton | 1/3 | 0.066(1) | 0.0079(3) |
| | 2/5 | 0.037(1) | 0.0090(11) |
| | 3/7 | 0.027(3) | 0.0095(32) |

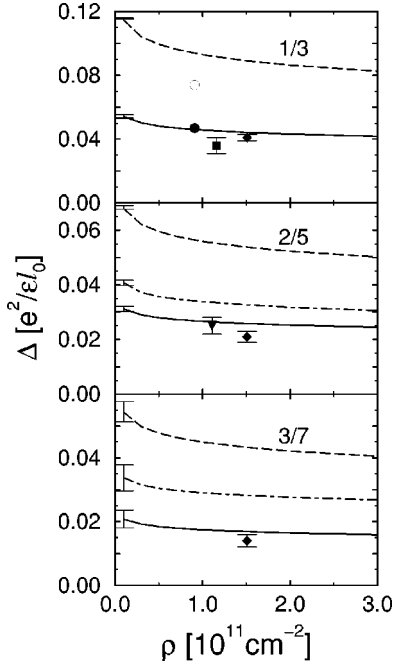


FIG. 5. The energies of the fundamental and the secondary rotons (solid and dash-dotted lines, respectively) and of the CF exciton in the long-wavelength limit (dashed line) as a function of the density for a heterojunction. Experimental energies are also shown, taken from Refs. 8 (circle), 9 (diamond), 10 (square), and 11 (down-triangle); the filled symbols correspond to the roton, and the empty ones to the long-wavelength mode.

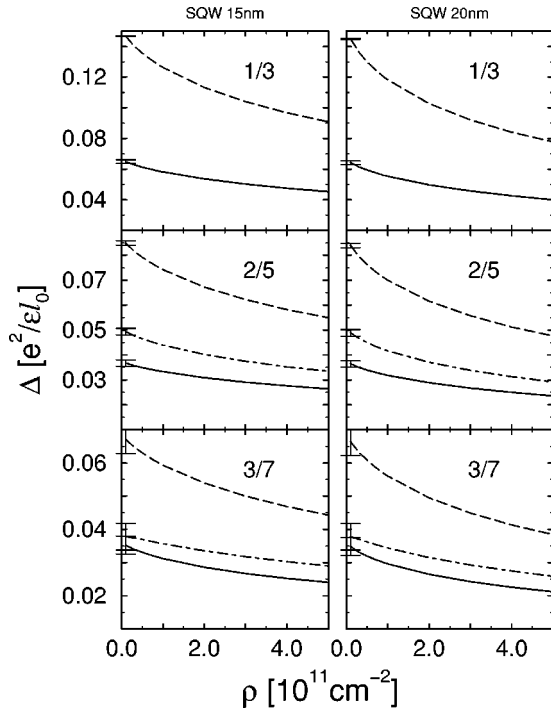


FIG. 6. The energies of the fundamental and the secondary rotons (solid and dash-dotted lines, respectively) and of the CF exciton in the long-wavelength limit (dashed line) as a function of density for the square-quantum-well geometry for two different quantum-well widths.

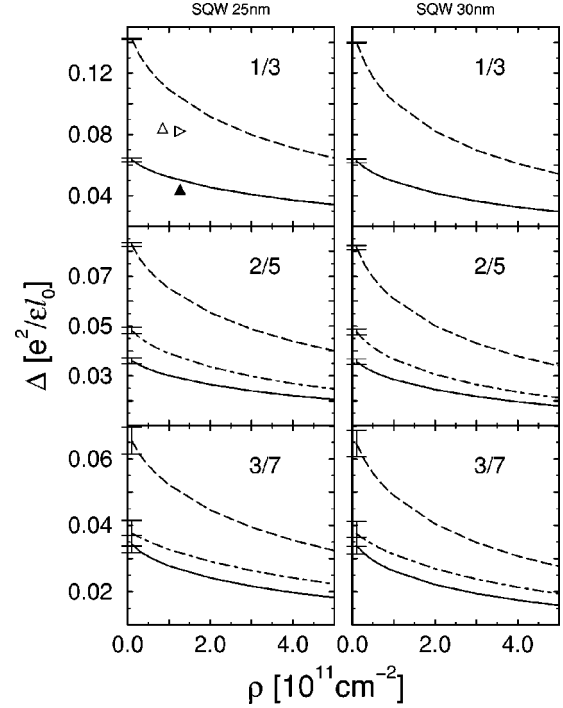


FIG. 7. Same as in Fig. 6 but for quantum wells of width 25 and 30 nm. The experimental results are taken from Refs. 5 (up-triangle) and 6 (right-triangle); the filled (empty) symbols correspond to the roton (long-wavelength mode).

obtained by fitting the points near the minimum to a parabolic dispersion

$$\Delta_k^{ex} = \Delta + \frac{\hbar^2(k - k_0)^2}{2m_R^*} \quad (30)$$

for each N , and then extrapolating Δ to the thermodynamic limit. We note that it becomes necessary to go to larger systems as the effective filling of composite fermions increases; for example, for $\nu = 3/7$, it was important to study up to 63

TABLE II. Comparison of theory and experiment for the roton energy as well as the energy of the long-wavelength exciton, quoted in units of $e^2/\epsilon l_0$. In Ref. 9, the roton energies were determined for $2/3$, $3/5$, and $4/7$, which, assuming particle-hole symmetry, are the same as the roton energies at $1/3$, $2/5$, and $3/7$, when measured in units of $e^2/\epsilon l_0$.

| ν | $kl_0=0$ | | Roton | | Reference |
|-------|------------|----------|------------|-----------|-----------|
| | experiment | theory | experiment | theory | |
| 1/3 | 0.082 | 0.104(1) | 0.044 | 0.050 (1) | 6 |
| | 0.084 | 0.113(1) | - | 0.052(1) | 5 |
| | - | 0.090(2) | 0.041(2) | 0.045(1) | 9 |
| | 0.074 | 0.095(1) | 0.047 | 0.047(1) | 8 |
| | - | 0.092(1) | 0.036(5) | 0.045(1) | 10 |
| 2/5 | - | 0.054(1) | 0.021(2) | 0.026(1) | 9 |
| | - | 0.055(1) | 0.025(3) | 0.027(1) | 11 |
| 3/7 | - | 0.044(2) | 0.014(2) | 0.017(2) | 9 |

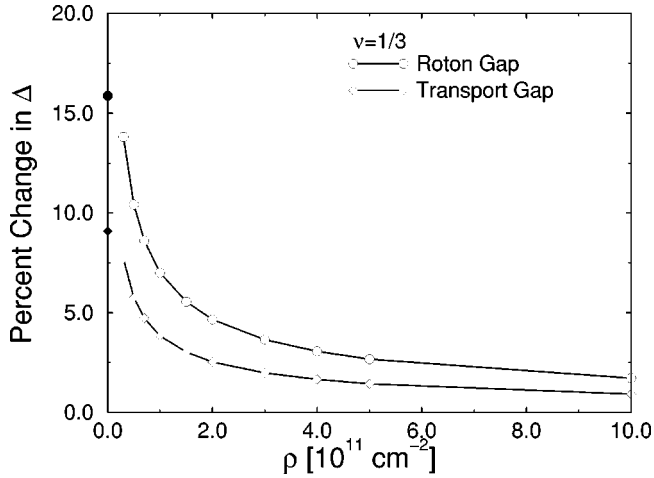


FIG. 8. The percent change in the energy due to Landau-level mixing both for the fundamental roton (upper curve) and the activation gap (lower curve) at $\nu=1/3$. The Landau-level mixing has been treated as explained in the text. The results correspond to the heterojunction geometry, for a ten-electron system. The filled symbols correspond to the pure Coulomb interaction.

particles to obtain a reliable thermodynamic estimate. The energies in the $kl_0 \rightarrow 0$ limit and at the roton minimum are given in Table I, along with m_R^* , for a strictly two-dimensional system, i.e., for the pure Coulomb interaction.

Figures 5, 6, and 7 plot the energy of the fundamental and a secondary CF roton and the long-wavelength CF exciton for heterojunction and square quantum-well geometries as a function of the density, with finite thickness effects included in self-consistent LDA, as discussed above. It also depicts the experimental energies determined from ballistic phonon absorption (at 1/3, 2/5, and 3/7) as well as in inelastic light scattering experiments (at 1/3). A more detailed comparison is given in Table II.

For the CF roton, the theoretical energies, obtained with no adjustable parameters, are in excellent agreement with the observed ones. One may worry that the situation will be spoiled by Landau-level mixing. This turns out not to be the case. As shown in Fig. 8, the LL-mixing corrections are on the order of 5–10% for typical densities, consistent with a similar conclusion for the transport gap.^{20,21} As mentioned earlier, the effect of Landau-level mixing on the gap diminishes fast as one goes from an ideal two-dimensional system to a realistic system with finite thickness. The high degree of agreement between theory and experiment also confirms that the roton energies are not as significantly affected by disorder as those of the charged excitations.

In the small-wave-vector limit, the experimental and theoretical energies at 1/3 are off by $\sim 30\%$. Given our experience with the roton, it is tempting to suspect that this discrepancy is real. Here, exact diagonalization studies indicate that the energy of the CF exciton comes close to other excitations, and it is likely that the energy of the CF exciton will be significantly lowered due to *composite-fermion*-LL mixing. Such a CF-LL mixing will occur through screening by other excitons, and is related to earlier suggestions^{12,36} that at small wave vectors the true lowest energy excitation may be a quadrupolar excitation containing a bound pair of *two* rotons. There has been debate as to which excitation is being

probed by the Raman scattering in this case.^{12,35} In exact diagonalization studies it has not been possible to obtain definitive information regarding these issues due to the rather small system sizes.

While the ballistic phonon absorption experiments directly measure the minimum energy (i.e., the energy of the fundamental roton),³⁶ the Raman experiments ideally probe the $kl_0 \rightarrow 0$ limit of the CF exciton dispersion, the wavelength of the light being much larger than l_0 . However, a breakdown of momentum conservation due to the presence of disorder can activate rotons as well,³⁷ as a result of a singularity in the density of states. This has been crucial in explaining multiple peaks in the Raman spectra for the inter-LL excitations. At $\nu=1/3$, a low-energy Raman peak has been interpreted as the roton.^{6,8} Recently, Kang *et al.*⁷ also observed modes at 2/5 and 3/7, at energies of $0.031e^2/\epsilon l_0$ and $0.008e^2/\epsilon l_0$, respectively, which they interpret as the long wavelength neutral mode. Our calculated energies at 2/5 and 3/7 for a quantum well of width 30 nm and density $\rho=5.4 \times 10^{10} \text{ cm}^{-2}$ are $0.031(3)e^2/\epsilon l_0$ and $0.021(3)e^2/\epsilon l_0$, respectively, for the roton, and $0.070(1)e^2/\epsilon l_0$ and $0.056(3)e^2/\epsilon l_0$ for the $kl_0=0$ CF exciton. At 2/5, the energy of the observed excitation is consistent not only with the calculated roton energy but also with those measured in ballistic phonon absorption experiments, and substantially smaller than the calculated $kl_0 \rightarrow 0$ limit, which might suggest an identification with the fundamental roton. We note here that the observation of the 1/3 roton implies that the violation of the momentum conservation is sufficiently widespread as to render the fundamental rotons at 2/5 and 3/7 observable as well, which occur at roughly the same wave vectors ($kl_0 \approx 1.6-1.7$) as the 1/3 roton ($kl_0 \approx 1.4$). The energy of the 3/7 mode of Ref. 7 is anomalously low, however. Further work will be required to ascertain the precise nature of these new Raman modes; an experimental observation of multiple peaks, possible due to the existence of several rotons and maxons, will be especially helpful in clarifying this issue.

IV. CONCLUSION

Our main conclusion is that the composite-fermion theory provides an excellent account of the observed energy of the CF roton with no adjustable parameters. This is possible because of the insensitivity of the roton energy to disorder.

ACKNOWLEDGMENTS

We are grateful to Professor Aron Pinczuk for communicating his results to us prior to publication and for the continuous exchange of information, and to Xiaomin Zu for numerous helpful discussions. This work was supported in part by the National Science Foundation under Grant No. DMR-9986806. We are grateful to the Numerically Intensive Computing Group led by V. Agarwala, J. Holmes, and J. Nucciarone at the Penn State University CAC for computing time and assistance at the LION-X cluster.

- ¹*Composite Fermions*, edited by Olle Heinonen (World Scientific, New York, 1998).
- ²*Perspectives in Quantum Hall Effects*, edited by S. Das Sarma and A. Pinczuk (Wiley, New York, 1997).
- ³J. K. Jain, Phys. Rev. Lett. **63**, 199 (1989); Phys. Rev. B **41**, 7653 (1990); J. K. Jain and R. K. Kamilla, in *Composite Fermions* (Ref. 1).
- ⁴D. C. Tsui, H. L. Stormer, and A. C. Gossard, Phys. Rev. Lett. **48**, 1559 (1982).
- ⁵A. Pinczuk, B. S. Dennis, L. N. Pfeiffer, and K. West, Phys. Rev. Lett. **70**, 3983 (1993); Semicond. Sci. Technol. **9**, 1865 (1994); A. Pinczuk, in *Perspectives in Quantum Hall Effects* (Ref. 2).
- ⁶A. Pinczuk, B. S. Dennis, L. N. Pfeiffer, and K. West, *Proceedings of 12th International Conference on High Magnetic Fields in Physics of Semiconductors* (World Scientific, Singapore, 1997), p. 83.
- ⁷Moonsoo Kang, A. Pinczuk, B. S. Dennis, M. A. Eriksson, L. N. Pfeiffer, and K. W. West, Phys. Rev. Lett. **84**, 546 (2000).
- ⁸H. D. M. Davies, J. C. Harris, J. F. Ryan, and A. J. Turberfield, Phys. Rev. Lett. **78**, 4095 (1997).
- ⁹C. J. Mellor, R. H. Eyles, J. E. Digby, A. J. Kent, K. A. Benedict, L. J. Challis, M. Henini, and C. T. Foxon, Phys. Rev. Lett. **74**, 2339 (1995).
- ¹⁰U. Zeitler, A. M. Devitt, J. E. Digby, C. J. Mellor, A. J. Kent, K. A. Benedict, and T. Cheng, Phys. Rev. Lett. **82**, 5333 (1999).
- ¹¹A. M. Devitt, S. H. Roshko, U. Zeitler, C. J. Mellor, A. J. Kent, K. A. Benedict, T. Cheng, and M. Henini, Physica E **5**, 47 (2000).
- ¹²S. M. Girvin, A. H. MacDonald, and P. M. Platzman, Phys. Rev. Lett. **54**, 581 (1985); Phys. Rev. B **33**, 2481 (1986).
- ¹³R. P. Feynman and M. Cohen, Phys. Rev. **102**, 1189 (1956).
- ¹⁴E. Manousakis and V. R. Pandharipande, Phys. Rev. B **30**, 5064 (1984).
- ¹⁵J. K. Jain and R. K. Kamilla, Phys. Rev. B **55**, R4895 (1997).
- ¹⁶J. K. Jain and R. K. Kamilla, Int. J. Mod. Phys. B **11**, 2621 (1997).
- ¹⁷R. L. Willett, H. L. Stormer, D. C. Tsui, A. C. Gossard, and J. H. English, Phys. Rev. B **37**, 8476 (1988).
- ¹⁸R. Morf, Phys. Rev. Lett. **83**, 1485 (1999).
- ¹⁹K. Park, N. Meskini, and J. K. Jain, J. Phys.: Condens. Matter **11**, 7283 (1999), and references therein.
- ²⁰V. Melik-Alaverdian and N. E. Bonesteel, Phys. Rev. B **52**, R17032 (1995).
- ²¹R. Price and S. Das Sarma, Phys. Rev. B **52**, 17 032 (1995); V. Melik-Alaverdian and N. Bonesteel, Phys. Rev. Lett. **79**, 5286 (1997).
- ²²For theory, see K. Park and J. K. Jain, Phys. Rev. Lett. **80**, 4237 (1998); **83**, 5543 (1999); X. G. Wu, G. Dev, and J. K. Jain, *ibid.* **71**, 153 (1993). For experiment, see R. R. Du, A. S. Yeh, H. L. Stormer, D. C. Tsui, L. N. Pfeiffer, and K. W. West, *ibid.* **75**, 3926 (1995); I. V. Kukushkin, K. v. Klitzing, and K. Eberl, *ibid.* **82**, 3665 (1999); S. Melinte, N. Freytag, M. Horvatić, C. Berthier, L. P. Lévy, V. Bayot, and M. Shayegan, Phys. Rev. Lett. **84**, 354 (2000).
- ²³A. Lopez and E. Fradkin, Phys. Rev. B **47**, 7080 (1993); S. H. Simon and B. I. Halperin, *ibid.* **48**, 17 368 (1993); X. C. Xie, *ibid.* **49**, 16 833 (1994).
- ²⁴G. Murthy, Phys. Rev. B **60**, 13 702 (1999).
- ²⁵F. D. M. Haldane, Phys. Rev. Lett. **51**, 605 (1983).
- ²⁶T. T. Wu and C. N. Yang, Nucl. Phys. B **107**, 365 (1976); Phys. Rev. D **16**, 1018 (1977). All quantities, including the wavefunctions and the kinetic energy, are written in gauge “a” of this reference.
- ²⁷F. Stern and S. Das Sarma, Phys. Rev. B **30**, 840 (1984); S. Das Sarma and F. Stern, *ibid.* **32**, 8442 (1985).
- ²⁸We obtain the uncertainty in the thermodynamic values for the gap, i.e., the y intercept of our linear χ^2 fit, using standard routines for estimating the variance via error propagation assuming that the data at each N are independent. For details, see W. H. Press, S. A. Teukolsky, W. T. Vetterling, and B. P. Flannery, *Numerical Recipes in C*, 2nd ed. (Cambridge University Press, Cambridge, 1992).
- ²⁹M. W. Ortalan, S. He, and S. Das Sarma, Phys. Rev. B **55**, 7702 (1997).
- ³⁰D. Ceperley, G. V. Chester, and M. H. Kalos, Phys. Rev. B **16**, 3081 (1977); S. Fahy, X. W. Wang, and S. G. Louie, *ibid.* **42**, 3503 (1990).
- ³¹R. Morf *et al.*, Phys. Rev. B **34**, 3037 (1986).
- ³²K. Park and J. K. Jain, cond-mat/9910460 (unpublished).
- ³³We note that at small wave vectors, for which the wavelength becomes comparable to the size of the sphere, a comparison between the results obtained in the finite-size spherical geometry (our Monte Carlo calculations) and those in the planar geometry (as in the SMA) is somewhat complicated by the finite-size effects. For this reason, it is more appropriate to compare both the GMP mode and the CF exciton energies for the same geometry, which is what we have done in case of $\nu=1/3$ (Fig. 1).
- ³⁴R. K. Kamilla, X. G. Wu, and J. K. Jain, Phys. Rev. B **54**, 4873 (1996).
- ³⁵P. M. Platzman and S. He, Phys. Rev. B **49**, 13 674 (1991).
- ³⁶K. A. Benedict, R. K. Hills, and C. J. Mellor, Phys. Rev. B **60**, 10 984 (1999).
- ³⁷A. Pinczuk, J. P. Valladares, D. Heiman, L. N. Pfeiffer, and K. W. West, Surf. Sci. **229**, 384 (1990).